photonics

Article

Planar Bilayer PT-Symmetric Systems and Resonance Energy Transfer

Aliaksandr Arlouski * and Andrey Novitsky *

Physics Faculty, Belarusian State University, Nezavisimosti Avenue 4, 220030 Minsk, Belarus
* Correspondence: av.arlouski@gmail.com (A.A.); novitsky@bsu.by (A.N.)

Abstract: Parity-time (PT) symmetry provides an outstanding improvement of photonic devices' performance due to the remarkable physics behind it. Resonance energy transfer (RET) as an important characteristic mediating the molecules that can be tailored in the PT-symmetric environment, too. We study how planar bilayer PT-symmetric systems affect the process of resonance energy transfer occurring in the vicinity thereof. First, we investigate the reflectance and transmittance spectra of such systems by calculating reflection and transmission coefficients as well as total radiation amplification as functions of medium parameters. We obtain that reflectance and total amplification are greatest near the exceptional points of the PT-symmetric system. Then, we perform numerical calculations of the RET rate and investigate its dependence on the complex permittivity of the PT-symmetric medium, dipole orientation, frequency of radiation and layer thickness. Optically thick PT-symmetric systems may operate at lower gain at the expense of the appearance of chaotic-like behaviors. These appear owing to the dense oscillations in the reflectance and transmittance spectra and vividly manifest themselves as stochastic-like positions of the exceptional points for PT-symmetric bilayers. The RET rate, being a result of the field interference, can be significantly amplified and suppressed near exceptional points exhibiting a Fano-like lineshape.

Keywords: PT-symmetry; exceptional points; resonance energy transfer; RET; reflection and transmission; planarly-layered medium

check for updates

Citation: Arlouski, A.; Novitsky, A. Planar Bilayer PT-Symmetric Systems and Resonance Energy Transfer. *Photonics* **2024**, *11*, 169. https://doi.org/10.3390/photonics11020169

Received: 18 January 2024
Revised: 2 February 2024
Accepted: 8 February 2024
Published: 10 February 2024

Copyright: © 2024 by the authors. Licensee MDPI, Basel, Switzerland. This article is an open access article distributed under the terms and conditions of the Creative Commons Attribution (CC BY) license (https://creativecommons.org/licenses/by/4.0/).

1. Introduction

In their 1998 paper, Bender and Boettcher conjectured that quantum–mechanical systems described by non-Hermitian Hamiltonians may, under certain conditions, possess entirely real-valued spectra [1]. For this, it is necessary and sufficient that its eigenfunctions are invariant under the action of parity-time (PT) operator [2]. Later, through the formal analogy between the stationary Schrödinger equation and the Helmholtz equation in electrodynamics, the concept of the PT symmetry migrated to optics [3–5]. By definition, an optical system is called PT-symmetric if its permittivity ε satisfies the following condition

$$\varepsilon^*(\mathbf{r}, \omega) = \varepsilon(-\mathbf{r}, \omega), \tag{1}$$

where $\mathbf{r}$ is the radius-vector, ω is the angular frequency of the incoming electromagnetic field and * denotes complex conjugation. Despite difficulties with experimental implementation [4], PT-symmetric systems have attained a great amount of interest, because they possess a number of peculiar properties, like double and asymmetric refraction in optical lattices and unidirectional invisibility [3,6]. Exceptional points play a tremendous part in non-Hermitian photonics, offering a new physics due to the interplay of the loss and gain components [7]. Recently, exceptional points were observed along a synthetic orbital angular momentum dimension [8] and were experimentally found above the lasing threshold due to the cavity detuning [9]. Perfectly chiral exceptional points were realized using the mirror-symmetry-broken metasurface through the chiral quasi-bound state in the continuum [10]. Higher-order exceptional points are able to enhance the sensibility of non-Hermitian sensors [11,12] due to the intriguing increase in the spectral response strength [13].

In the present work, we explore the influence of spectral properties of optically thick bilayer PT-symmetric systems on the process of resonance energy transfer (RET). Resonance energy transfer is a quantum–electrodynamic process of non-radiative energy transfer between two quantum systems, one of which, initially in an excited state (donor), releases a virtual photon, which is subsequently absorbed by another system, initially in the ground state (acceptor). As was originally shown by Förster using semi-classical approximation [14], the RET rate depends on the distance R between the donor and acceptor as R^{-6}, being very short ranged. Nevertheless, it plays an important role in the energy exchange between organic molecules [15]. The RET rate increases near the exceptional points; the greater the order of the exceptional point, the larger the RET rate [16].

This paper is organized as follows. Section 1 contains an introduction. In Section 2, we calculate and analyze the power reflection r and transmission t coefficients of planar PT-symmetric bilayers as functions of layer thickness for different values of loss and gain and investigate their behavior for the case of optically thick layers. We relate the maxima of reflectance and total intensity of the scattered radiation with the exceptional points of PT-symmetric systems. In Section 3, we carry out numerical calculations of the spectral density function $T(\omega)$ that defines the effect of the environment on the RET rate and study its correlation to the exceptional points. In Section 4, we discuss the obtained results. Section 5 concludes the paper.

2. Reflective and Transmissive Properties of Planar PT-Symmetric Media

2.1. General Remarks

Figure 1a illustrates the simplest example of a planar medium satisfying the PT-symmetry condition (1). It consists of two bulks of the same thickness L and permittivities $\varepsilon' + i\varepsilon''$ and $\varepsilon' - i\varepsilon''$ of lossy and gain media, respectively. An obvious generalization, illustrated in Figure 1b, is a periodic planar system comprising N layers, the permittivities of which are equal to $\varepsilon_j = \varepsilon' + (-1)^{j+1}\, i\varepsilon''$, $j = 1, \ldots, N$.

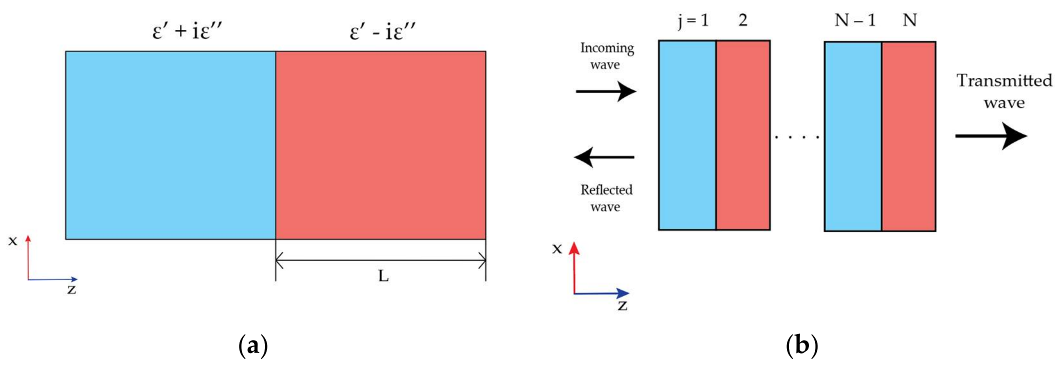

Figure 1. (**a**) A bilayer planar PT-symmetric system. (**b**) A periodic planar PT-symmetric system composed of N layers.

Before proceeding further, we would like to briefly mention three points. The first one is the fact that the definition of PT-symmetric media depends on the choice of a coordinate frame: its origin has to be placed at the interface between two layers in Figure 1a to satisfy Equation (1). Obviously, it makes little sense for a system to be PT-symmetric in one set of coordinates and not to be such in another. Therefore, any system composed of alternating loss and gain layers of equal thickness, such that the absolute value of ε'' is the same for each layer, will be referred to as being PT-symmetric. The second point concerns the negative sign of ε'', that is, the gain. If plane waves are described by $\exp[i(\mathbf{kr} - \omega t)]$, then the electromagnetic radiation propagating through a layer with $\varepsilon'' < 0$ is being exponentially amplified. Any amplification requires a mechanism that provides a source of energy for the propagating wave, and a negative imaginary part of ε is an effective macroscopic way of describing this mechanism [17]. The examples of such a mechanism are the stimulated emission of radiation and coupling to an external gain source. The amplified radiation may greatly affect the properties of the medium, including permittivity ε, to the point when amplification may disappear altogether. The precise intensity of radiation at which this happens has to be determined either experimentally or from the microscopic properties of the system under study. In what follows, we assume that the value of the permittivity is unaffected by the propagating radiation. Finally, the last point concerns the frequency dependence of ε. Complex permittivity is fundamentally related to the dispersive properties of media [17] and, strictly speaking, we need to remember that permittivity depends on the frequency ω of the incoming radiation. It was shown in [4], using the Kramers–Kronig relations, that the PT-symmetry condition, defined by Equation (1), holds only for a discrete set of frequencies. Thus, it makes sense to perform all the calculations for some fixed frequency ω (or wavelength λ), assuming that the system is PT-symmetric at that frequency. In Section 2.2, when we plot the dependencies versus L/λ, it is implied that the thickness of layers L rather than the wavelength λ is being varied.

In the next subsection, we investigate power reflection r and transmission t coefficients of PT-symmetric layered systems. Along with them, we calculate $r+t$, which shows how the total intensity of the incoming radiation changes after interacting with the layered system. Since a medium with $\varepsilon'' \neq 0$ can both amplify and absorb the incoming radiation, there is no reason for $r+t$ to be equal to 1, as in the case of pure dielectrics, or to decay exponentially, as in the case of pure metals. Instead, a complex interplay between loss, gain and interference effects takes place, which leads to non-trivial results.

2.2. Calculations and Discussion

The derivation of r and t coefficients is presented in Appendix A. The power coefficients are defined as the moduli squared of the diagonal elements of the matrices (A9) and (A10); the latter generalize the Fresnel coefficients. Since we consider the case of normal incidence and all layers are isotropic, the power reflection and transmission coefficients are the same for TE- and TM-polarized modes. We distinguish two cases for the bilayer system In Figure 1a: (i) the incoming wave hits the gain layer first and (ii) it hits the loss layer first. Once the real part of the permittivity $\mathrm{Re}(\varepsilon)$ and geometry of the system are fixed, there are only three essential parameters to vary: the thickness of layer L, wavenumber of the incoming wave k and imaginary part of the dielectric permittivity ε''. Noticing that the wavenumber and thickness appear only as a product $kL = 2\pi L/\lambda$ in the definition of the reflection and transmission coefficients (see Appendix A), it makes sense to investigate the dependence of r and t coefficients on the ratio L/λ, i.e., on the thickness, measured in the units of wavelength of the incoming wave. We take $\varepsilon' = 3$ and consider four values of ε'', namely, $0.03,\ 0.05,\ 0.1$ and 0.3. The results for r and t coefficients are presented in Figures 2 and 3. The plots look solid, but in fact they are highly oscillatory with a period $\propto \mathrm{Re}\big(1/\sqrt{\varepsilon}\big)$. In Figure 4, we investigate asymptotic behavior $L/\lambda \to \infty$ (that is, the case of very thick layers) of $r+t$ with respect to ε'' for different values of ε'.

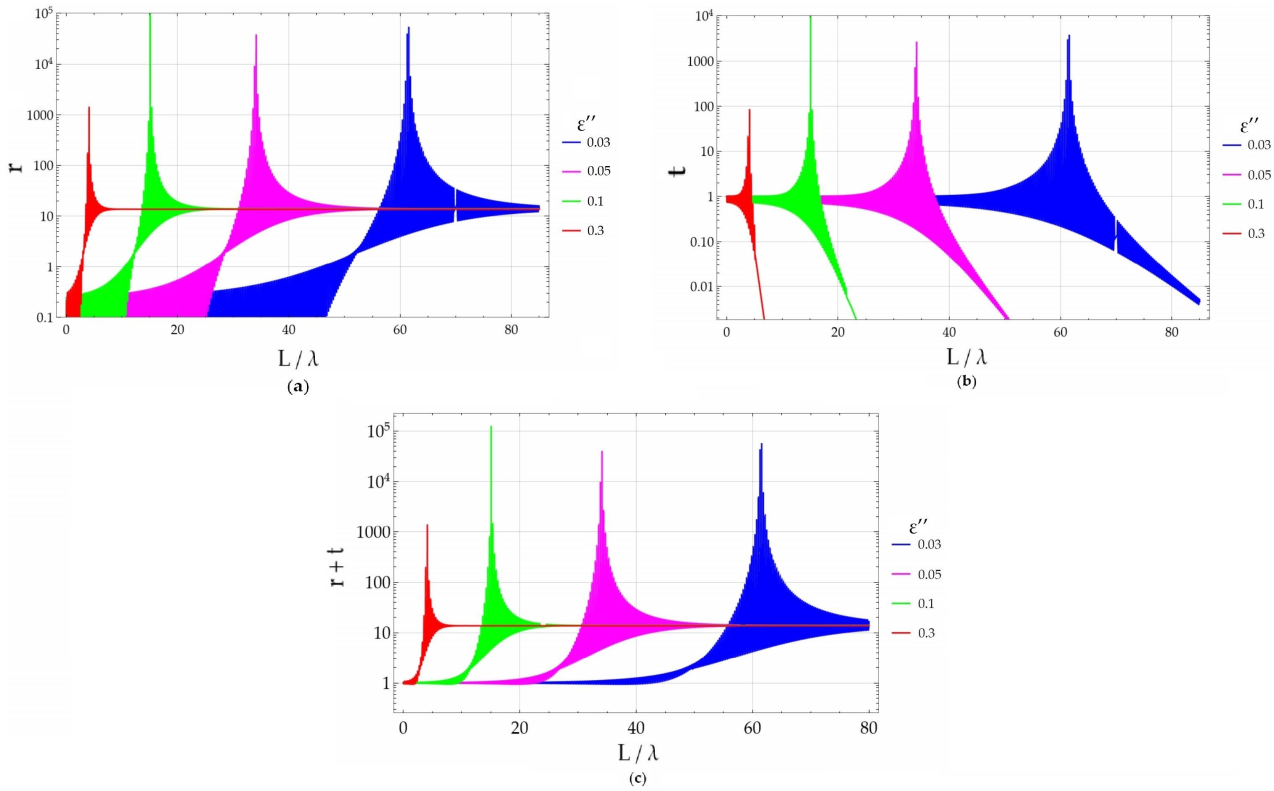

Figure 2. (**a**) Reflectance, (**b**) transmittance and (**c**) total intensity gain in the 'gain slab'–'loss slab' sequence of layers.

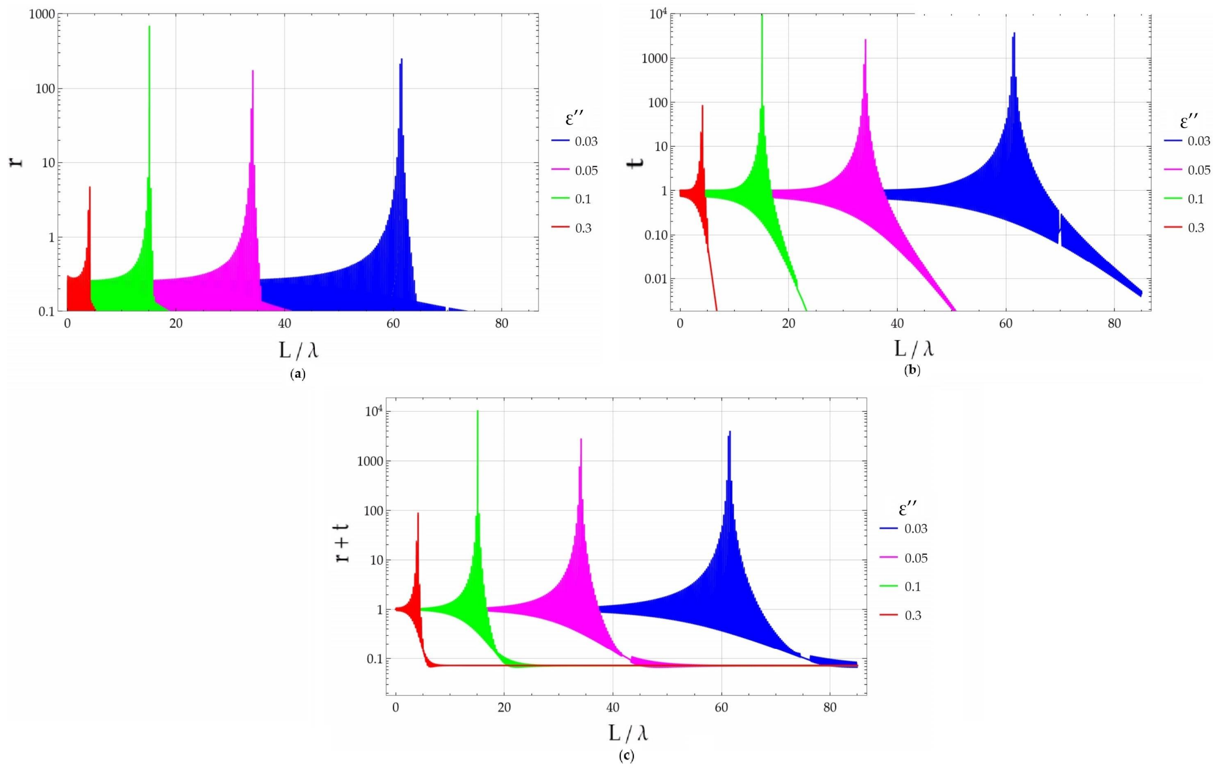

Figure 3. (**a**) Reflectance, (**b**) transmittance and (**c**) total intensity gain in the 'loss slab'–'gain slab' sequence of layers.

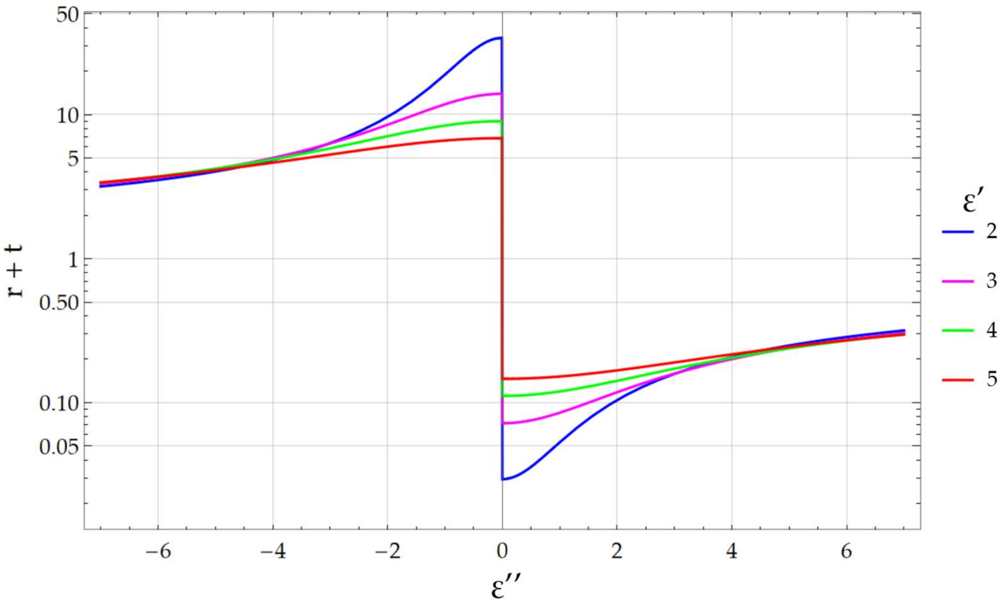

Figure 4. Asymptotic behavior of $r + t$ at $L/\lambda \to \infty$.

The first thing one observes when comparing Figures 2 and 3 is the obvious fact that the order of loss and gain layers matters. Being reciprocal, the system has the same transmittance independent of the order of layers; however, the reflectance is drastically different.

In both cases of layer ordering, there exists a layer thickness, at which the reflectance, transmittance and intensity amplification have sharp spikes. When the gain layer meets the electromagnetic wave first, the maximum amplification is greater than in the case of the opposite sequence of layers by about an order of magnitude (cf. Figures 2a and 3a). Although, as the calculation shows, the maximum amplification reaches the values 10^4–10^5 in one case and 10^3–10^4 in the other, one should keep in mind that these values are likely unattainable in practice due to the arguments noted in Section 2.1. One may still expect that a spike of amplification (most probably, less pronounced) will be observed in the actual experiment near the layer thicknesses predicted by the theory. In any case, the practical realization of the two-layer system under study requires fine tuning due to the highly oscillatory nature of r and t.

Transmittance (Figures 2c and 3c) is the same in both cases of layer ordering: at small values of L/λ (precisely which values are 'small' is different for different permittivities), the larger part of the incoming radiation passes through the medium; then, t has a sharp spike, after which it quickly decreases to zero. However, the behavior of reflectance is qualitatively different for the two cases. If the loss layer is placed first, r is almost zero for small L/λ; then, it has a sharp spike, after which it drops to small but non-vanishing values. If, instead, the gain layer is placed first, then at large L/λ, it does not fall off but rather remains near 10. The asymptotic behavior of $r + t$ (effectively r alone, since for large L/λ, transmittance quickly vanishes in both cases) illustrated in Figure 4 has the following properties:

- It depends significantly on the permittivity of the first layer: if the gain layer is first, then there is a net intensity gain, while if the loss layer is first, then the intensity is absorbed rather than amplified.
- The smaller the value of $\mathrm{Re}(\varepsilon)$ at $\varepsilon'' < 0$ ($\varepsilon'' > 0$), the larger (smaller) the asymptotic intensity gain $r + t$.
- The total intensity gain $r + t$ tends to 1 for very large values of $|\varepsilon''|$.

We also notice that for large values of L/λ, the amplitude of oscillations of both r and t significantly decreases. Thus, if one aims at constructing a layered PT-symmetric system with a given level of amplification, it is more expedient to use thick layers with the value of ε'' which provides the desired level of amplification. Although the asymptotic amplification is much smaller than the maximum amplification, the former is substantially easier to achieve, since no fine tuning is required.

Having investigated the reflective and transmissive properties of the bilayer PT-symmetric system, the next step is to investigate how these properties affect the RET rate. In particular, it is interesting to check whether there is an amplification of RET rate at the points of maximum reflection and whether the asymptotic behavior of r manifests itself in the asymptotic behavior of the RET rate. But before proceeding further, let us relate the obtained spectral properties to the exceptional points of the PT-symmetric system in question.

2.3. Connection to Exceptional Points

In the context of photonics, the exceptional points of a multilayer PT–symmetric system are defined through the analysis of the eigenvalues of the scattering matrix (S-matrix) [18]. The eigenvalues of the scattering matrix are normally complex numbers of absolute value equal to one. However, by tailoring the system's parameters (for example, ε'' and layer thickness L), one is able to approach an exceptional point, where the system undergoes a PT symmetry breaking [19], and the absolute value of each eigenvalue is not the unity anymore. For example, consider the bilayer system in Figure 1a characterized by parameters $\mathrm{Re}(\varepsilon) = 3$ and $L = 7.5$ µm, which scatters the incoming radiation of wavelength 500 nm. For the ratio $L/\lambda = 15$, an exceptional point appears at $\mathrm{Im}(\varepsilon) \approx 0.09$ (see Figure 5). Here, we use the S-matrix eigenvalues of the form $\lambda_{1,2} = (R_L + R_R)/2 \pm \sqrt{1 - (R_L + R_R)^2/4}$, where R_L and R_R are, respectively, the field reflection-to-the left and reflection-to-the-right coefficients [18].

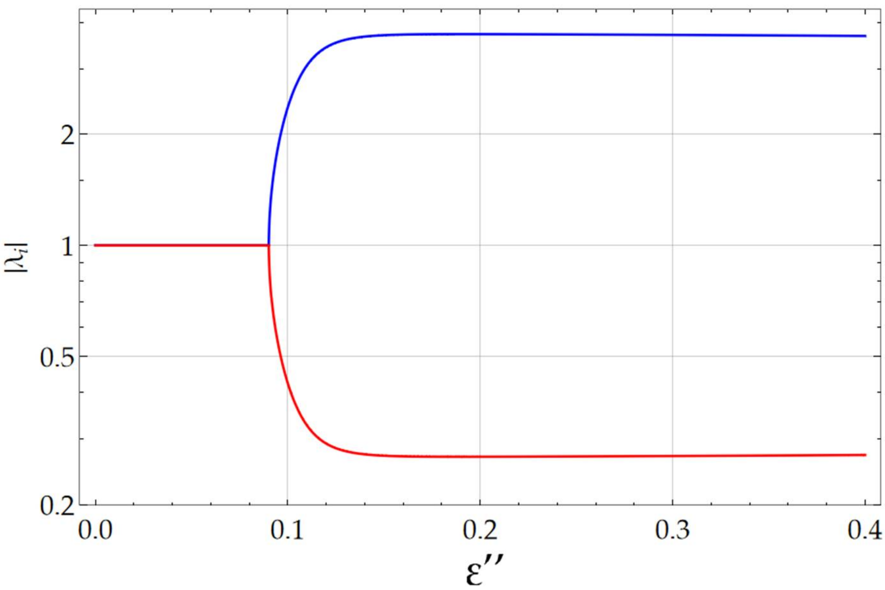

Figure 5. Absolute value of the eigenvalues of the S-matrix. Red and blue colors refer to two different eigenvalues. Notice the log scale on the $|\lambda_i|$ axis. Parameters: $\mathrm{Re}(\varepsilon) = 3$, $L = 7.5$ µm and $\lambda = 500$ nm.

From Figures 2 and 3, we notice that the r and t power coefficients have a sharp spike at approximately $L/\lambda = 15$ when $\varepsilon'' = 0.1$, i.e., the spikes in Figures 2 and 3 are related to the exceptional points of the bilayer system defined by $(R_L + R_R)^2/4 = 1$. Exactly in this case, the eigenvalues of the S-matrix coalesce, $\lambda_1 = \lambda_2$. As discussed in Ref. [18], the exceptional points of the multilayer system can be introduced twofold. The first-type exceptional point corresponds to the transfer from the regime of balanced loss and gain to the regime of imbalanced loss and gain. An exceptional point of the second type (considered in our manuscript) is a lasing predictor, in the vicinity of which the instability is developed, while the reflectance and transmittance take large but finite values. The reflectance enhancement can be also expected from the exceptional point condition $R_L + R_R = \pm 2$, which says that the reflectance becomes great and has a tendency to increase. The locations of the exceptional points in the $(\varepsilon'', L/\lambda)$ coordinates are presented in Figure 6 as blue dots. For all the considered values of $\mathrm{Im}(\varepsilon)$ from Figures 2 and 3, the spikes correspond to the exceptional points in Figure 6. The positions of the blue points in Figure 6 are not sufficiently regular, though they are concentrated in the vicinity of the fitting curve of the form $y(x) = a + bx^{-1} + cx^{-2}$, where a, b and c are constants. Irregularity can be associated with dense oscillations in the spectral reflection and transmission dependences, when a tiny variation of the thickness L/λ results in the great change in the reflectance and transmittance. The stochastic-like positions of points in Figure 6 is a manifestation of the dynamic chaos known in the theory of dynamic systems. The picture shown in Figure 6 is a result of a particular discretization of the normalized length L/λ (similar discretization can be performed for ε''). Such a chaotic-like nature imposes restrictions on the experimental realization of the PT-symmetric systems with predicted behaviors.

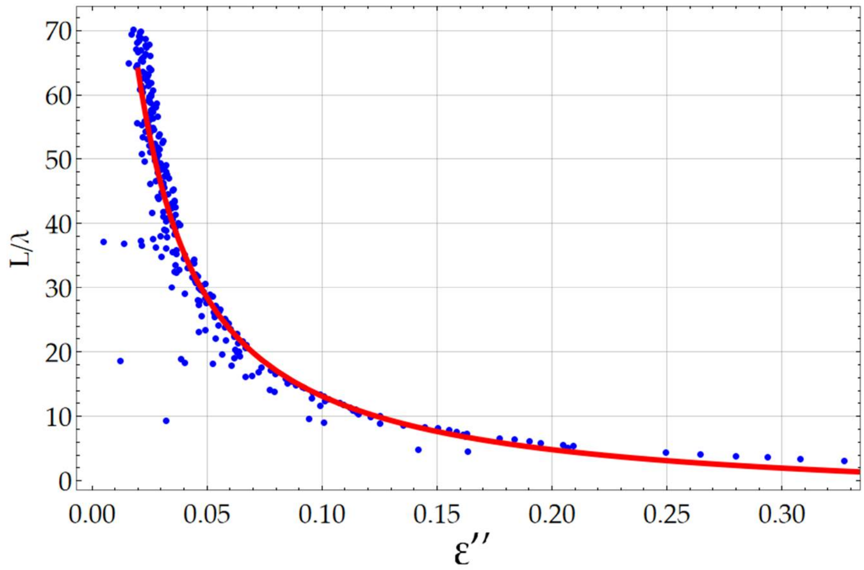

Figure 6. Exceptional points (blue points) in $(\mathrm{Im}(\varepsilon), L/\lambda)$ coordinates. Red curve approximates the location of points with $y(x) = a + bx^{-1} + cx^{-2}$, where $a \approx -3.91$, $b \approx 1.79$ and $c \approx 8.75 \cdot 10^{-3}$ are constants obtained using least-squares fit.

3. Resonance Energy Transfer in the Presence of a Bilayer PT-Symmetric Medium

The rate of the resonance energy transfer is given by the relationship [20]

$$\gamma_{D\to A} = \int_0^\infty \sigma_{em}(\omega)\sigma_{abs}(\omega)T(\omega)d\omega, \tag{2}$$

where $\sigma_{em}(\omega)$ and $\sigma_{abs}(\omega)$ are the donor luminescence and acceptor absorption spectra, respectively, and the spectral function

$$T(\omega) = \frac{2\pi}{\hbar^2}\left(\frac{\omega^2}{\varepsilon_0 c}\right)^2 |\mathbf{d}_\mathrm{D} G(\omega, \mathbf{r}_\mathrm{D}, \mathbf{r}_\mathrm{A})\mathbf{d}_\mathrm{A}|^2. \tag{3}$$

Here, G is the dyadic Green's function of the system (see Appendix B), $\mathbf{d}_\mathrm{A}$ and $\mathbf{d}_\mathrm{D}$ are the electric dipole moments of, respectively, the acceptor and donor, $\mathbf{r}_\mathrm{A}$ and $\mathbf{r}_\mathrm{D}$ are their radius-vectors, and ω is the angular frequency associated with the released photon. From Equation (3), one can immediately deduce that Green's function specifies the dependence of the RET rate on the surrounding environment. Since PT-symmetric media may both amplify and absorb radiation depending on the wavelength and layer thickness, one could expect a similar kind of behavior when calculating the RET rate. However, it is hard to tell a priori which values of the parameters of the system correspond to amplification or attenuation because of the aforementioned interplay of loss, gain and interference effects.

The configuration of the system we consider is as follows (see Figure 7): two quantum systems with electric dipole moments $\mathbf{d}_A = d_A\mathbf{n}_A$ and $\mathbf{d}_D = d_D\mathbf{n}_D$ ($\mathbf{n}_{A,D}$ are unit vectors) are placed inside a semi-infinite medium with $\varepsilon = 1$ (air or vacuum) near the interface of a bilayer PT-symmetric medium. The parameters that determine the intensity of the RET rate are shown in Figure 7:

- Magnitudes of the dipole moments $d_{A,D}$ and orientations of the unit vectors $\mathbf{n}_{A,D}$.
- Distances z_A and z_D from, respectively, acceptor and donor to the interface.
- Lateral separation $r_\perp$ between the donor and acceptor systems.
- Wavelength λ of the mediated photon.
- Permittivity ε and thickness L of layers.

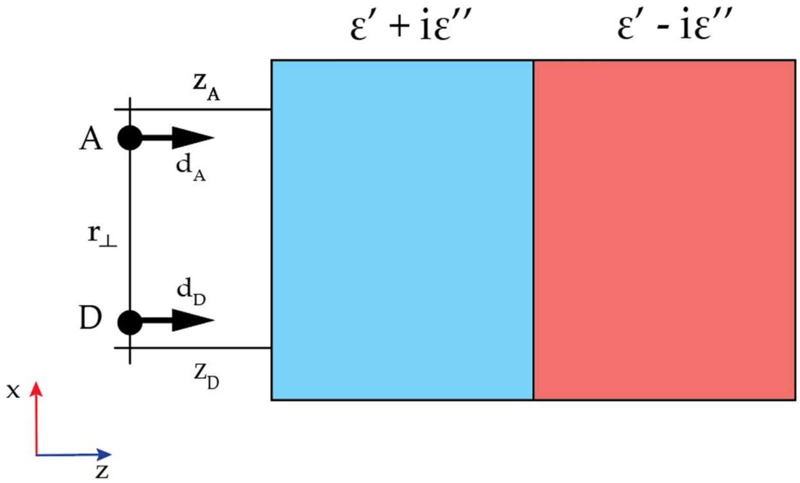

Figure 7. Configuration of the system under study when the dipoles are oriented along the z-axis.

We want to compare the RET rate with and without the layered medium (in the latter case, both dipoles are surrounded by vacuum). To that end, the exact values of $d_{A,D}$ are irrelevant, since they cancel out in the ratio of spectral functions T/T_0. The parameters take the following values: $\lambda = 500$ nm, $z_A = z_D = \lambda/10 = 50$ nm and $r_\perp = \lambda/50 = 10$ nm. As in Section 2, we consider four values of ε'' : 0.03, 0.05 ,0.1 and 0.3.

The results are presented in Figures 8 and 9 for the two cases when both dipoles are oriented along either z or x-axis, respectively.

We see that the dependence of the spectral function T on L/λ roughly resembles that of the intensity gain (cf. Figures 2a and 3a). The positions of the spikes in Figures 8 and 9 correspond to those in Figures 2 and 3. This means that the RET rate is directly correlated with the scattering properties of the surrounding environment and in the case of the PT-symmetric layered system, it is greatest at the exceptional points.

When the gain layer is placed first, one observes a significant amplification of the spectral function T owing to the electromagnetic energy concentration in the gain slab, while when the loss layer is placed first, the amplification is scarce and barely noticeable for all thicknesses except for the chosen ones (see Figures 8 and 9). The asymptotic behavior is similar to that in Figures 2 and 3: the order of loss and gain layers matters. The asymptotic amplification is substantial only if the gain layer is placed first. It is worth noting that even when the loss layer is placed first, the spectral function in the PT-symmetric environment is still slightly amplified (cf. Figure 4, where radiation is attenuated when $\mathrm{Im}(\varepsilon) > 0$). The increase in T is of the same order of magnitude for both orientations of dipoles.

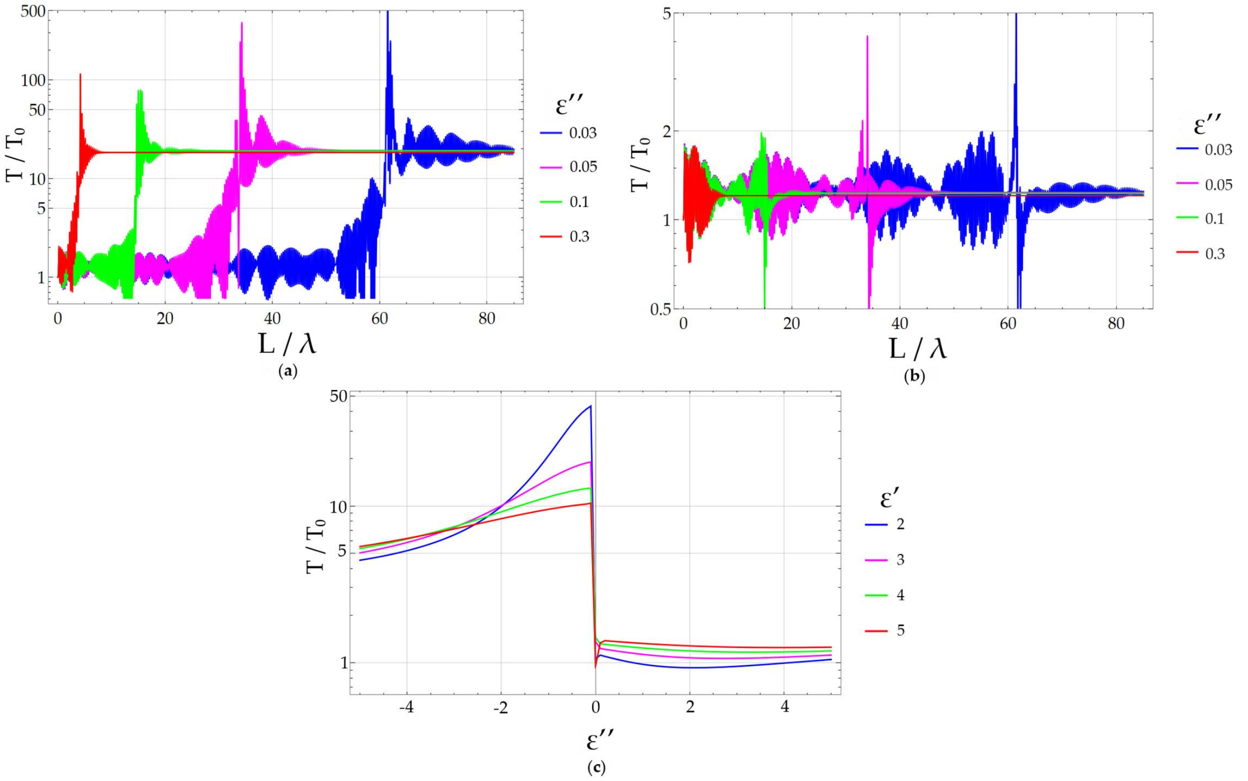

Figure 8. Ratio of the spectral function near the PT-symmetric medium T to the spectral function in vacuum T_0 for dipoles oriented along the z-axis. (**a**) Gain layer is placed first; (**b**) loss layer is placed first; (**c**) asymptotic behavior at $L \to \infty$.

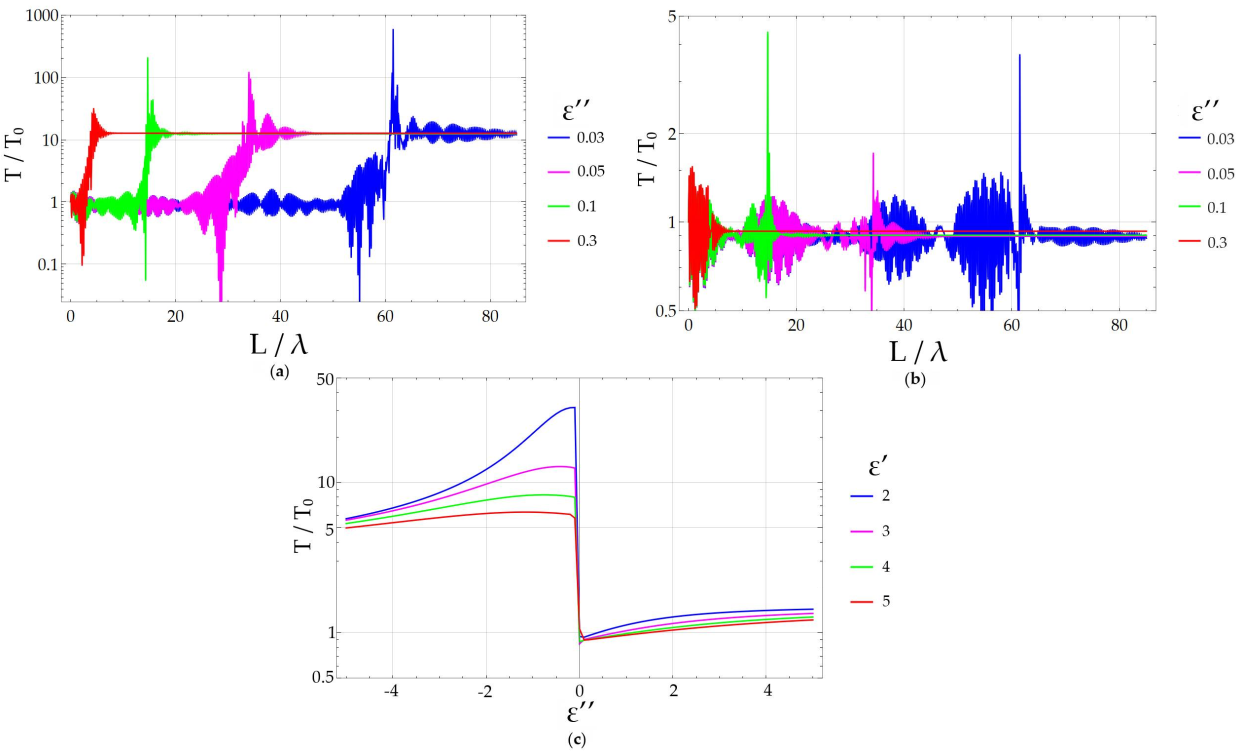

Figure 9. Ratio of the spectral function rate in vicinity of the PT-symmetric medium T to the spectral function in vacuum T_0 for dipoles oriented along the x axis. (**a**) Gain layer is placed first; (**b**) loss layer is placed first; (**c**) asymptotic behavior at $L \to \infty$.

According to Ref. [16], the spectral density function $T(\omega)$ maximizes in the vicinity of the exceptional point, though it may depart from the exact position of the exceptional point due to the perturbation caused by dipoles. In Figures 8 and 9, we also observe suppression of the spectral density T to the values below T_0. The availability of the enhancement and suppression is explained by the interference of two electromagnetic fields, the first of which propagates directly from the donor to the acceptor, while the second field originates from the reflection at the layer interface. Near the exceptional point in the loss–gain configuration: both strong enhancement and strong suppression are realized, resembling a Fano lineshape.

4. Discussion

All the results presented above have been obtained using numerical calculations. While performing these calculations, we used the following assumptions: (1) no matter how high the radiation amplification in a PT-symmetric medium, the material parameters remain the same; (2) the value of the RET rate is given by expressions (4) and (5); (3) the presence of dipoles does not modify the environment. The validity of the first assumption has to be determined either experimentally or using the microscopic theory of the PT-symmetric medium under study, as discussed in Section 2.1. The amplitudes of waves in the experiments aimed at determining the reflective properties of media are by far not sufficient to alter their characteristics, so this assumption is justified. (Such an experiment may be realized, for example, by placing a sample of medium inside a waveguide connected to a vector network analyzer). For the second assumption to be valid, the dipole approximation has to be true, since it played a key role in the derivation of Equation (2) (see [20]). This means that the quantity kd is sufficiently small, where k is the wavenumber of the emitted photon and d is the characteristic size of the donor and acceptor. Moreover, all the characteristic length scales in the problem should be sufficiently greater than interatomic distances, so that the effective macroscopic treatment of medium using dyadic Green's function is applicable. Finally, the third assumption is not strictly true, since the presence of dipoles should at least slightly modify the environment, resulting in the departure from the perfect PT symmetry of the considered system. The perturbation theory can be exploited in order to account for the RET more accurately, as seen in [16]. The perturbation changes the positions of the exceptional points as well as Green's function and the RET rate in the vicinity of exceptional points. Thus, the maximum of the spectral function $T(\omega)$ shifts. However, the RET rate as an integral (4) will include all frequencies, and the effect of the maximum displacement will likely not be dramatic, being exhibited as a perturbative correction.

The shape of the spectral function amplification curves resembles a Fano lineshape, which is a result similar to that obtained in Ref. [20], where the RET rate between two molecules located near a planar dielectric half-space was calculated as a function of the transition frequency. There, the maximum amplification rate is of the order 10^2, which is a result similar to ours. However, a PT-symmetric environment causes residual amplification in the asymptotic case of thick layers (or, alternatively, in the case of short wavelengths of mediated photons), which is a result that is absent when a dielectric half-space is considered.

The numerically obtained maximum amplification of the spectral function is of the order 10^2. It is reasonable to ask whether it is experimentally possible to obtain such levels of amplification. In Ref. [21], the authors report an amplification of the RET rate by a factor of 10^2, but it was achieved by placing the donor and acceptor inside a dielectric particle of diameter $\approx$10 μm rather than by placing them near a layered medium. The recent study on the RET rate near a planar metasurface reports an amplification by a factor of 1–10 depending on the geometry of the experiment [22]. This level of amplification is lower than that obtained in the present paper, but the experiment was conducted in the microwave range, whereas we took the wavelength of the mediated photon to be in the optical (500 nm) range. While various experimental difficulties may prevent the achievement of the RET rate amplification by a factor of 10^2, this possibility should not be discarded on a priori grounds.

It is possible to predict the location of amplification spikes in bilayer PT-symmetric systems using the obtained results. To that end, one needs to construct the scattering matrix of such a system, calculate its eigenvalues for some set of parameters and, by varying parameters separately, determine the points of bifurcation; the obtained points are approximately the desired points of maximum spectral amplification and RET rate. But, unfortunately, due to the highly oscillatory behavior of reflection and transmission coefficients, even in the case of an ideal bilayer medium, the procedure described above may require serious fine tuning. In general, optically thick PT-symmetric systems demonstrate a chaotic-like behavior clearly exhibiting itself in the positions of exceptional points and in 'noisy' curves for the spectral function of the RET rate. Interestingly, both strong enhancement and strong suppression near the exceptional points are available. Oscillations also decay as the thickness of layers increases, which means no fine tuning is required if thick layers are chosen in the experiment setup. Thus, instead of trying to achieve maximum amplification at the location of exceptional points, it might be more expedient to obtain a lesser but stably predictable amplification in the asymptotic (large L) case. To that end, one only has to numerically determine which values of ε'' produce the desired asymptotic behavior of $T(\omega)$ and use the materials with the obtained parameters in an experiment.

Although we did not study multilayered systems with the number of layers $N > 2$ herein, it is natural to ask what would differ in that case. Moreover, one could ask how the obtained results would change in the case of non-planar (e.g., spherical or cylindrical) and/or anisotropic PT-symmetric media. To encompass such systems, the appropriate Green functions should be determined. Since the set of systems allowing the closed-form Green functions is limited, the numerical methods of finding the Green functions might be used. Perhaps it is natural to conjecture that a behavior similar to that observed in the present paper is also true for such systems, i.e., the location of amplification spikes corresponds to the location of the exceptional points of PT-symmetric systems. In any case, these non-trivial questions deserve a separate study.

5. Conclusions

We have numerically investigated the reflective and transmissive properties of a bilayer PT-symmetric system paying attention to its influence on the resonance energy transfer rate between the donor and acceptor quantum systems. The main results are as follows:

- The order of loss and gain layers matters greatly: it affects both the total intensity gain and RET rate amplification for a given thickness of layers and the asymptotic amplification at $L \to \infty$.
- In the 'gain slab'–'loss slab' sequence of layers (Figure 2), the maximum reflection and amplification is of the order 10^5, while in the opposite sequence of layers (Figure 3), the maximum reflection and amplification is of the order 10^4, which is an order of magnitude lower. The asymptotic amplification (Figure 4) is of the order 10 in the 'gain slab'–'loss slab' case (radiation is amplified) and of the order 0.1 in the 'loss slab'–'gain slab' case (radiation is attenuated).
- The pattern of the spectral function amplification T/T_0 of the RET rate resembles that of the intensity gain and reflection: whenever the radiation is highly amplified and reflected, the RET rate also rises.
- In the 'gain slab'–'loss slab' sequence of layers, the maximum RET spectral function amplification is of the order 100 and the asymptotic amplification is around 20, while in the opposite sequence of layers, the amplification is barely noticeable: maximum amplification is of the order of unity, and asymptotic amplification is practically absent (Figures 8 and 9). These results are true for both orientations of the dipole moments (whether along the z or x-axis).
- The reflection and amplification of radiation by PT-symmetric systems are greatest at the values of media parameters corresponding to the exceptional points of such

systems. Hence, if there is a PT-symmetric medium located near interacting dipoles, then the RET rate is also greatest at the exceptional points.

Author Contributions: A.A.: conceptualization, theoretical analysis, numerical calculations. A.N.: conceptualization, theoretical analysis, draft review. All authors have read and agreed to the published version of the manuscript.

Funding: A.N. acknowledges the support of the State Program for Scientific Research "Convergence-2025" (Task 2.1.02.1).

Institutional Review Board Statement: Not applicable.

Informed Consent Statement: Not applicable.

Data Availability Statement: The results and details of numerical calculations may be obtained from authors upon request.

Conflicts of Interest: The authors declare no conflicts of interest.

Appendix A. Derivation of the Reflection and Transmission Coefficients

The details and subtleties of the derivation presented below (including the case of anisotropic and bianisotropic media) can be found in [23]; here, we present a sketch of the derivation and summarize the results for isotropic media.

Consider a planar layered medium made of N isotropic layers with permittivities $\hat{\varepsilon}_j = \varepsilon_j \mathbf{1}$, where ε_j are (complex) constants and $\mathbf{1}$ is the identity operator (see Figure 1b). The z-axis is the direction of stratification. For plane waves, the Maxwell equations reduce to

$$\frac{\mathrm{d}\mathbf{W}}{dz} = ikM\mathbf{W}, \tag{A1}$$

$$\begin{gathered} \mathbf{W} = \begin{pmatrix} \mathbf{H}_t \\ \mathbf{q}\times\mathbf{E} \end{pmatrix},\ \mathbf{H}_t = \begin{pmatrix} H_x \\ H_y \end{pmatrix},\ \mathbf{q}\times\mathbf{E} = \begin{pmatrix} E_y \\ -E_x \end{pmatrix},\ M = \begin{pmatrix} A & B \\ C & D \end{pmatrix}, \\ A = D = \begin{pmatrix} 0 & 0 \\ 0 & 0 \end{pmatrix},\ B = \varepsilon\mathbf{e}_y\otimes\mathbf{e}_y + (\varepsilon - b^2)\mathbf{e}_x\otimes\mathbf{e}_x, \\ C = I - (b^2/\varepsilon)\mathbf{e}_y\otimes\mathbf{e}_y, \end{gathered} \tag{A2}$$

where $\mathbf{e}_x$, $\mathbf{e}_y$ and $\mathbf{q} = \mathbf{e}_z$ are the unit vectors along the respective axes, I is the projector onto the xy-plane (unit two-dimensional matrix), $\otimes$ is the tensor (or Kronecker) product, $k = \omega/c$ is the wavenumber in vacuum and $b \equiv |\mathbf{b}|$ is defined so that $k\mathbf{b}$ is the tangential component of the wavevector $\mathbf{k}$ lying in the xy-plane. Note that since $\mathbf{H}_t$ and $\mathbf{q}\times\mathbf{E}$ are field projections onto the xy-plane, we treat them as two-dimensional vectors. Hence, M is a 4×4 rather than 6×6 block matrix. The full three-dimensional fields can be restored using the known tangential fields, as it is shown in [23].

The solution to Equation (A1) in a homogeneous medium can be written in terms of the evolution operator Ω as

$$\mathbf{W}(z) = \mathrm{e}^{ikM(z-z_0)}\mathbf{W}(z_0) \equiv \Omega_{z_0}^{z}\mathbf{W}(z_0). \tag{A3}$$

The wave travels smoothly within each layer. Moreover, it is well known that tangential components of electromagnetic field vectors are continuous at the interface of two media. Hence, the tangential components of the fields at the first interface, where the incoming wave hits the system, and at the $(N+1)$-th interface, where the outgoing wave leaves it, are connected in the following way:

$$\mathbf{W}^{(N+1)} = \Omega_{z_0}^{z_N}\mathbf{W}^{(0)},\ \Omega_{z_0}^{z_N} = \Omega_{z_{N-1}}^{z_N}\ldots\Omega_{z_0}^{z_1}. \tag{A4}$$

Tangential components of the fields are related via the so-called surface impedance tensor γ: $\mathbf{q}\times\mathbf{E} = \gamma\mathbf{H}_t$. Tensor γ depends on the material parameters of the medium and tangential component $\mathbf{b}$ of the wavevector. If the wave propagates in the direction opposite to $\mathbf{q}$ (the reflected wave), then γ gains the minus sign. Let γ_0 and γ_{N+1} be the surface impedance tensors of the semi-infinite media, which surround the layered system. (If the system under investigation is surrounded by vacuum and the incidence is normal, which we assume is the case, then γ_0 and γ_{N+1} are simply 2×2 unit matrices.) Noting that the field at the 0-th interface is composed of the incoming and reflected parts, we may write the following equations:

$$\begin{gathered} \mathbf{W}^{(0)} = \mathbf{W}^{(inc)} + \mathbf{W}^{(ref)},\ \mathbf{W}^{(inc)} = \begin{pmatrix} I \\ \gamma_0 \end{pmatrix} \mathbf{H}_{\mathrm{t}}^{(inc)}, \\ \mathbf{W}^{(ref)} = \begin{pmatrix} I \\ -\gamma_0 \end{pmatrix} \mathbf{H}_{\mathrm{t}}^{(ref)},\ \mathbf{W}^{(n+1)} \equiv \mathbf{W}^{(tr)} = \begin{pmatrix} I \\ \gamma_{N+1} \end{pmatrix} \mathbf{H}_{\mathrm{t}}^{(tr)}, \end{gathered} \tag{A5}$$

where *inc*, *ref* and *tr* stand for 'incoming', 'reflected' and 'transmitted'. Substituting (A5) into (A4) yields

$$\begin{pmatrix} I \\ \gamma_{N+1} \end{pmatrix} \mathbf{H}_{\mathrm{t}}^{(tr)} = \Omega_{z_0}^{z_N} \left[\begin{pmatrix} I \\ \gamma_0 \end{pmatrix} \mathbf{H}_{\mathrm{t}}^{(inc)} + \begin{pmatrix} I \\ -\gamma_0 \end{pmatrix} \mathbf{H}_{\mathrm{t}}^{(ref)} \right]. \tag{A6}$$

Now, we introduce dyadic (matrix) reflection and transmission coefficients R and T:

$$\mathbf{H}_{\mathrm{t}}^{(ref)} = R\mathbf{H}_{\mathrm{t}}^{(inc)},\ \mathbf{H}_{\mathrm{t}}^{(tr)} = T\mathbf{H}_{\mathrm{t}}^{(inc)}. \tag{A7}$$

The substitution of (A7) into (A6) results in the following system of equations:

$$\begin{pmatrix} I \\ \gamma_{N+1} \end{pmatrix} T = \Omega_{z_0}^{z_N} \left[\begin{pmatrix} I \\ \gamma_0 \end{pmatrix} + \begin{pmatrix} I \\ -\gamma_0 \end{pmatrix} R \right]. \tag{A8}$$

Multiplying it by the 2×4 block matrix $\begin{pmatrix} \gamma_{N+1} & -I \end{pmatrix}$ from the left side, one can readily see that the 2×2 matrix reads

$$R = -\left[\begin{pmatrix} \gamma_{N+1} & -I \end{pmatrix} \Omega_{z_0}^{z_N} \begin{pmatrix} I \\ -\gamma_0 \end{pmatrix} \right]^{-1} \left[\begin{pmatrix} \gamma_{N+1} & -I \end{pmatrix} \Omega_{z_0}^{z_N} \begin{pmatrix} I \\ \gamma_0 \end{pmatrix} \right]. \tag{A9}$$

In a similar manner, noting that $\left(\Omega_{z_0}^{z_N}\right)^{-1} = \Omega_{z_N}^{z_0}$, one obtains the expression for the 2×2 matrix T as

$$T = 2\left[\begin{pmatrix} \gamma_0 & I \end{pmatrix} \Omega_{z_N}^{z_0} \begin{pmatrix} I \\ \gamma_{N+1} \end{pmatrix} \right]^{-1} \gamma_0. \tag{A10}$$

The 2×2 matrices R and T are diagonal for the stack of isotropic media. The moduli squared of the diagonal elements are the power reflection and transmission coefficients for TE and TM modes, which is what we sought.

Thus, the process of finding r and t reduces to the construction of the evolution operator $\Omega_{z_0}^{z_N}$, surface impedance tensor γ_i and performing matrix operations. If all parameters, like permittivity, frequency, etc. are fixed, then this is relatively easy to do. However, if one needs to investigate the dependence of r and t coefficients on the mentioned parameters, calculations quickly become very exhausting (especially when considering oblique incidence) and are usually only possible to perform with the help of a computer.

Appendix B. Dyadic Green's Function

A thorough discussion of the applications of Green's functions to layered media can be found in [24].

Given a differential equation

$$L\mathbf{W}(\mathbf{r}) = \mathbf{J}(\mathbf{r}), \tag{A11}$$

where L is a differential operator and $\mathbf{W}$, $\mathbf{J}$ are vector functions, Green's function G is defined as an operator inverse to L as

$$LG\left(\mathbf{r},\mathbf{r}'\right) = \delta\left(\mathbf{r}-\mathbf{r}'\right)\mathbb{1}. \tag{A12}$$

Here, $\delta(\boldsymbol{r}-\boldsymbol{r}')$ is the Dirac's delta function. Using Green's function, the solution to (A11) is given by

$$\mathbf{W}(\mathbf{r}) = \mathbf{W}_0(\mathbf{r}) + \int_V G\left(\mathbf{r},\mathbf{r}'\right)\mathbf{J}\left(\mathbf{r}'\right)d^3,\ L\mathbf{W}_0(\mathbf{r}) = 0, \tag{A13}$$

the integration being restricted to the volume, where the source term $\mathbf{J}(\mathbf{r})$ does not vanish and $\mathbf{W}_0$ being chosen such that boundary conditions are respected. Furthermore, we assume that the following restrictions hold:

- The system is stationary, i.e., the time dependence is described by the factor $e^{-i\omega t}$.
- The medium is non-magnetic ($\mu = 1$).
- The fields are produced due to the electric current equivalent to dipole oscillation with frequency ω as follows $\mathbf{j}(\mathbf{r}) = -i\omega\mathbf{d}\ \delta(\mathbf{r}-\mathbf{r}_0)$, where $\mathbf{d}$ is an electric dipole moment and $\mathbf{r}_0$ specifies the position of the dipole.

Upon applying the Lorenz gauge $\nabla\cdot\mathbf{A} = \frac{i\varepsilon\omega}{c}\varphi$, it is easy to obtain the following equation from Maxwell's equations:

$$(\Delta + k^2\varepsilon)\mathbf{A}(\mathbf{r}) = -4\pi ik\mathbf{d}\delta(\mathbf{r}-\mathbf{r}_0), \tag{A14}$$

where Δ is the Laplacian and $k = \omega/c$ is the wavenumber in vacuum. Its solution reads as [24,25]

$$\mathbf{A}(\mathbf{r}) = 4\pi ik\mathbf{d}g_0(\mathbf{r},\mathbf{r}_0), \tag{A15}$$

where $g_0(\mathbf{r},\mathbf{r}_0)$ is the scalar Green's function, having the form of a spherical wave:

$$g_0(\mathbf{r},\mathbf{r}_0) = \frac{\exp\left(ik\sqrt{\varepsilon}R\right)}{4\pi R} \tag{A16}$$

with $R \equiv |\mathbf{r}-\mathbf{r}_0|$. (If ε is a complex-valued quantity, then one should choose the square root with a positive real part.) From Equation (A15), the Lorenz gauge and the relations connecting the electric field and the electromagnetic potentials, one obtains

$$\mathbf{E} = 4\pi k^2 G_0(\mathbf{r},\mathbf{r}_0)\mathbf{d}, \tag{A17}$$

where

$$G_0\left(\mathbf{r},\mathbf{r}'\right) = \left(\mathbb{1} + \frac{1}{k^2\varepsilon}\nabla\otimes\nabla\right)g_0(\mathbf{r},\mathbf{r}'). \tag{A18}$$

is the dyadic Green's function. Here, $(\nabla\otimes\nabla)_{ij} \equiv \partial_i\partial_j$.

Despite it being straightforward to evaluate the action of $\nabla\otimes\nabla$ on g_0 (see [25] for details), it is more expedient to express Equation (A18) as a superposition of plane waves, i.e., to perform a Fourier transform of g_0. That will allow for separating TE and TM modes and then applying the Fresnel coefficients when dealing with the boundary-value problem. The plane wave decomposition of a spherical wave (A16) is the so-called Weyl identity [25]:

$$\frac{\exp\left(ik\sqrt{\varepsilon}R\right)}{4\pi R} = \frac{i}{8\pi^2}\int d^2\mathbf{k}_\perp \frac{\exp\left[i\left(\mathbf{k}_\perp\mathbf{R}_\perp + k_z\left|z-z'\right|\right)\right]}{k_z}, \tag{A19}$$

where because of the dispersion relation, $k_z = \sqrt{k^2\varepsilon - k_x^2 - k_y^2}$, and $\mathbf{k}_\perp$ and $\mathbf{R}_\perp$ are the components of the wavevector and the radius vector perpendicular to the z axis. Substituting Equation (A19) into Equation (A18) and noticing that $\partial_z^2 \left| z - z' \right| = 2\delta(z - z')$, we obtain

$$\begin{aligned} G_0(\mathbf{r}, \mathbf{r}') &= -\mathbf{e}_z \otimes \mathbf{e}_z \frac{\delta(\mathbf{r}-\mathbf{r}')}{k^2\varepsilon} + \frac{i}{8\pi^2} \int d^2\mathbf{k}_\perp \frac{1}{k_z} \left(1 - \frac{\mathbf{k}\otimes\mathbf{k}}{k^2\varepsilon}\right) e^{i\mathbf{kR}}, \\ \mathbf{k} &= \begin{cases} k_x \mathbf{e}_x + k_y \mathbf{e}_y + k_z \mathbf{e}_z, & z > z' \\ k_x \mathbf{e}_x + k_y \mathbf{e}_y - k_z \mathbf{e}_z, & z < z' \end{cases} \end{aligned} \tag{A20}$$

Note that $\mathrm{Re}(G_0)$ contains the delta function, which means that it diverges at $\mathbf{r} = \mathbf{r}'$, whereas $\mathrm{Im}(G_0)$ is generally finite. This fact is crucial when calculating, for example, the density of states (DOS), which requires the evaluation of $\mathrm{Im}(G_0(\mathbf{r}, \mathbf{r}))$. If, however, ε is complex, then both imaginary and real parts pick up the delta function and, hence, they both diverge. But since the calculation of RET rate requires the evaluation of G_0 at different spatial points corresponding to the donor and acceptor molecule positions, no singularities are present.

Equation (A20) is valid only for a homogeneous medium. The next step is to apply boundary conditions at the interfaces. This step is quite tedious: the resulting expressions are cumbersome and usually cannot be expressed in the closed form. The total dyadic Green's function is of the form

$$G(\mathbf{r}, \mathbf{r}_0) = \begin{cases} G_0 - \frac{c}{8\pi^2\omega\varepsilon_0\varepsilon^*} G^{(ref)}, & z \geq 0 \\ -\frac{c}{8\pi^2\omega\varepsilon_0\varepsilon} G^{(tr)}, & z < 0 \end{cases} \tag{A21}$$

The explicit expressions can be found in [26].

References

1. Bender, C.M.; Boettcher, S. Real Spectra in Non-Hermitian Hamiltonians Having PT Symmetry. *Phys. Rev. Lett.* **1998**, *80*, 5243–5246. [CrossRef]
2. Bender, C.M. Making sense of non-Hermitian Hamiltonians. *Rep. Prog. Phys.* **2007**, *70*, 947–1018. [CrossRef]
3. Makris, K.G.; El-Ganainy, R.; Christodoulides, D.N.; Musslimani, Z.H. Beam Dynamics in PT-Symmetric Optical Lattices. *Phys. Rev. Lett.* **2008**, *100*, 103904. [CrossRef] [PubMed]
4. Zyablovsky, A.A.; Vinogradov, A.P.; Pukhov, A.A.; Dorofeenko, A.V.; Lisyansky, A.A. PT-Symmetry in Optics. *Phys. Uspekhi.* **2014**, *184*, 1177–1198. [CrossRef]
5. El-Ganainy, R.; Makris, K.G.; Christodoulides, D.N.; Musslimani, Z.H. Theory of coupled optical PT-symmetric structures. *Opt. Lett.* **2007**, *32*, 2632–2634. [CrossRef] [PubMed]
6. Lin, Z.; Ramezani, H.; Eichelkraut, T.; Kottos, T.; Cao, H.; Christodoulides, D.N. Unidirectional Invisibility Induced by PT-Symmetric Periodic Structures. *Phys. Rev. Lett.* **2011**, *106*, 213901. [CrossRef] [PubMed]
7. Mohammad-Ali, M.; Andrea, A. Exceptional points in optics and photonics. *Science* **2019**, *363*, eaar7709. [CrossRef]
8. Yang, M.; Zhang, H.Q.; Liao, Y.W.; Liu, Z.H.; Zhou, Z.W.; Zhou, X.X.; Xu, J.S.; Han, Y.J.; Li, C.F.; Guo, G.C. Realization of exceptional points along a synthetic orbital angular momentum dimension. *Sci. Adv.* **2023**, *9*, eabp8943. [CrossRef]
9. Ji, K.; Zhong, Q.; Ge, L.; Beaudoin, G.; Sagnes, I.; Raineri, F.; El-Ganainy, R.; Yacomotti, A.M. Tracking exceptional points above the lasing threshold. *Nat. Commun.* **2023**, *14*, 8304. [CrossRef]
10. Zhou, Z.; Jia, B.; Wang, N.; Wang, X.; Li, Y. Observation of Perfectly-Chiral Exceptional Point via Bound State in the Continuum. *Phys. Rev. Lett.* **2023**, *130*, 116101. [CrossRef]
11. Chen, W.; Özdemir, S.K.; Zhao, G.; Wiersig, J.; Yang, L. Exceptional points enhance sensing in an optical microcavity. *Nature* **2017**, *548*, 192–196. [CrossRef] [PubMed]
12. Hodaei, H.; Hassan, A.U.; Wittek, S.; Garcia-Gracia, H.; El-Ganainy, R.; Christodoulides, D.N.; Khajavikhan, M. Enhanced sensitivity at higher-order exceptional points. *Nature* **2017**, *548*, 187–191. [CrossRef] [PubMed]
13. Wiersig, J. Moving along an exceptional surface towards a higher-order exceptional point. *Phys. Rev. A* **2023**, *108*, 033501. [CrossRef]
14. Förster, T. Zwischenmolekulare Energiewanderung und Fluoreszenz. *Ann. Phys.* **1948**, *437*, 55–75. [CrossRef]
15. Jones, G.A.; Bradshaw, D.S. Resonance Energy Transfer: From Fundamental Theory to Recent Applications. *Front. Phys.* **2019**, *7*, 100. [CrossRef]
16. Novitsky, A.; Morozko, F.; Gao, D.; Gao, L.; Karabchevsky, A.; Novitsky, D.V. Resonance energy transfer near higher-order exceptional points of non-Hermitian Hamiltonians. *Phys. Rev. B* **2022**, *106*, 195410. [CrossRef]
17. Landau, L.; Lifshitz, E. *Electrodynamics of Continuous Media*, 2nd ed.; Butterworth-Heinemann: Oxford, UK, 1984.

18. Novitsky, A.; Lyakhov, D.; Michels, D.; Pavlov, A.A.; Shalin, A.S.; Novitsky, D.V. Unambiguous scattering matrix for non-Hermitian systems. *Phys. Rev. A.* **2020**, *101*, 043834. [CrossRef]
19. Özdemir, Ş.; Rotter, S.; Nori, F.; Yang, L. Parity–time symmetry and exceptional points in photonics. *Nat. Mater.* **2019**, *18*, 783–798. [CrossRef]
20. Dung, H.T.; Knöll, L.; Welsch, D.-G. Intermolecular Energy Transfer in the Presence of Dispersing and Absorbing Media. *Phys. Rev. A* **2002**, *65*, 043813. [CrossRef]
21. Folan, L.M.; Arnold, S.; Druger, S.D. Enhanced energy transfer within a microparticle. *Chem. Phys. Lett.* **1985**, *118*, 322–327. [CrossRef]
22. Lezhennikova, K.; Rustomji, K.; Kuhlmey, B.T.; Antonakakis, T.; Jomin, P.; Glybovski, S.; de Sterke, C.M.; Wenger, J.; Abdeddaim, R. Experimental evidence of Förster energy transfer enhancement in the near field through engineered metamaterial surface waves. *Commun. Phys.* **2023**, *6*, 229. [CrossRef]
23. Borzdov, G.N. Frequency domain wave splitting techniques for plane stratified bianisotropic media. *J. Math. Phys.* **1997**, *38*, 6328–6366. [CrossRef]
24. Chew, W.C. *Waves and Fields in Inhomogeneous Media*; Wiley-IEEE Press: Hoboken, NJ, USA, 1999.
25. Novotny, L.; Hecht, B. *Principles of Nano-Optics*, 2nd ed.; Cambridge University Press: Cambridge, UK, 2012.
26. Cho, M.H.; Cai, W. Efficient and Accurate Computation of Electric Field Dyadic Green's Function in Layered Media. *J. Sci. Comp.* **2016**, *71*, 1319–1350. [CrossRef]

Disclaimer/Publisher's Note: The statements, opinions and data contained in all publications are solely those of the individual author(s) and contributor(s) and not of MDPI and/or the editor(s). MDPI and/or the editor(s) disclaim responsibility for any injury to people or property resulting from any ideas, methods, instructions or products referred to in the content.